Removal of Pb²⁺ and Zn²⁺ using modified Chocolate B clay: a study using statistical analysis, equilibrium isotherms, and adsorption kinetics

J. D. Mota¹, R. S. S. Cunha¹, M. G. F. Rodrigues¹*

¹Federal University of Campina Grande, Center of Sciences and Technology, Academic Unit of Chemical Engineering, R. Aprígio Veloso 882, 58429-970, Campina Grande, PB, Brazil

Abstract

In this work, natural and thermally modified Chocolate B clays were used for batch adsorption of Pb²⁺ and Zn²⁺ from an aqueous solution. The materials were characterized by X-ray diffraction, X-ray fluorescence spectroscopy, nitrogen adsorption, and cation exchange capacity. The tests were performed in a finite bath following a 2^2 factorial design, with the variables: pH and initial concentrations of metal. Results revealed that the thermal treatment caused alterations on the Chocolate B clay structure and decreased the specific surface area. Affinities between Pb²⁺ or Zn²⁺ and Chocolate B clay were found with adsorption capacities up to 3.36 and 3.72 mg.g⁻¹, respectively. The maximum adsorption capacities were 6.79 mg.g⁻¹ for Pb²⁺ and 3.35 mg.g⁻¹ for Zn²⁺ using thermally activated clay. The Langmuir and Freundlich models were used for the adsorption equilibrium analysis, and the Langmuir model provided the best fit for sorption isotherms. The adsorption kinetics was evaluated by two models: pseudo-first-order and pseudo-second-order. The pseudo-first-order kinetic model represented well the mechanism of interaction involved during Pb²⁺ adsorption into the pores of the clay. However, the two models represented well the mechanism of interaction of Zn²⁺ adsorption into the pores of the clay.

Keywords: Chocolate B clay, thermal activation, lead, zinc, sorption, isotherm, kinetics.

INTRODUCTION

Mining, smelting, and metal industry for manufacturing alloys are important economic activities. However, mining-related industries are also some of the largest sources of environmental pollution from heavy metals. Thus, in accordance with economic growth, the mining and processing of these metals have markedly increased during the last decades. Lead and zinc are important metals used in industrial activities. A large amount of lead, zinc, and related elements, such as cadmium, have been released into the environment due to mineral processing activities and have impacted water resources, soil, vegetables, and crops. In some areas, this pollution is hazardous to human health [1-4]. Mining and batteries are the main sources of heavy metal (Pb and Zn) contamination [3, 4]. Heavy metals are not biodegradable nor chemically destroyed, but must be treated before being discharged into the environment [5]. Several different procedures for removing metals from wastewater have been developed, such as chemical precipitation, ion exchange, and adsorption, among others. However, the high cost associated with most of these methods has become a limiting factor in its utilization [6].

Today, adsorption has become a promising choice for the treatment of heavy metals from wastewater. Adsorption is a solid-liquid mass transfer operation, where the heavy metal (adsorbate) is migrated from the wastewater to a solid surface (adsorbent) and then bonded to the adsorbent surface, due to chemical or physical adsorption [7]. This process is a greener and more sustainable alternative to other conventional technologies. The major benefits associated with adsorption are cost-effectiveness, high efficiency, regeneration of the adsorbent, low consumption of reagents, and the possibility of metal recovery [8]. Several alternative adsorptive materials have emerged, in the search to remove contaminants as efficiently as possible. Some reported adsorbents include: TiO₂ nanoparticles modified with poly(amidoamine) dendrimer [9], amino-functional poly(propylene imine) (PPI, G5) dendrimer linked silica (PPI/SiO₂) [10], poly(amidoamine) (PAMAM) dendrimers (generation 4: G4) [11], Fe₃O₄ magnetic nanoparticles [12], nanoparticles [13], and ZIF-8 [14]. The use of clay to remove the heavy metals present in effluents has been studied by various authors due to its economic advantages [15-18]. Clay materials, therefore, have important advantages when compared with other conventional adsorbents (zeolite, active coal, resins), which include: higher adsorption capacity, low cost, non-toxicity, high potential for ion exchange, high availability, and high specific surface area [19]. Clays and their minerals are abundant and cheap materials successfully used for decades as an adsorbent for removing toxic heavy metals from aqueous solutions [20, 21]. According to some studies [22, 23], the thermally modified clays are efficient for removing metal ions from the aqueous medium. Since water cleaning is one of the significant challenges worldwide, the use of cheap, eco-friendly, and local materials could be critical to improving water quality in the future.

Therefore, the objective of the present work was to thermally activate and characterize the Chocolate B clay

*meiry.rodrigues@ufcg.edu.br
https://orcid.org/0000-0003-2258-4230

and then determine the potential for removing Pb^{2+} and Zn^{2+} from an aqueous stream by sorption, analyzing the initial concentration and pH. Percentage of removal and removal capacity responses were examined, as well as the best settings for observing Langmuir and Freundlich isothermal models. Kinetic adsorption models were used to analyze kinetics. The present work represents a valuable platform for the development of material preparation (thermally activate clay) for future application of the adsorbent in pellets, that would be mechanically more resistant or avoid the possible flooding of the treatment columns due to the particle size of the materials.

MATERIALS AND METHODS

Adsorbent: Chocolate B clay from Boa Vista, in the State of Paraíba, Brazil, was provided by Bentonisa - Bentonite Nordeste. Clay was sieved using a Brazilian ABNT standard mesh 200 (0.074 mm) sieve. Then the sieved clay was thermally treated using a temperature-controlled muffle furnace. The sample was submitted to the following heat treatment: heating from room temperature until 500 °C with a controlled heating rate of 5 °C.min^{-1} and then 24 h of soaking time. The thermal treatment of the clay was carried out in order to increase its material stability, eliminate some impurities and ion exchange capacity [24]. The thermal treatment temperature and time were defined from the results of the thermogravimetry [25].

Characterization: Chocolate B clays, natural and thermally modified at 500 °C, were analyzed using a diffractometer (XRD 6000m, Shimadzu) with copper Kα radiation, operated at 30 mA and 40 kV, a goniometer velocity of 2 °/min and a step of 0.02° in the 2θ scanning range from 2° to 50°. The chemical composition was determined using X-ray fluorescence spectroscopy (XRF) with an energy dispersion spectrophotometer (EDX-700X-ray, Shimadzu). Nitrogen adsorption: the textural characteristics of the analyzed samples were investigated using isothermal gas adsorption/desorption of N_2 at 77 K (ASAP 2020, Micromeritics). The cation exchange capacity (CEC) was determined using the Kjeldahl method [26] with a Kjeldahl distiller (MA-036 Plus, Marconi).

Factorial experiment design: the combined effect of initial metal concentration and pH (natural and thermally activated Chocolate B clays) was investigated by a statistical experimental design (2^2 factorial design). pH plays an important role in the process of adsorption of heavy metal cations by clay minerals as it affects the behavior of heavy metal cations [27]. Chen et al. [28] reported an abrupt increase in sorption rate from 35% to 80% with an increase of pH from 2 to 4. An even better adsorption rate was observed as pH increased from 4 to 8, after which it became constant. A similar trend was observed by others [29-31]. The effect of initial pH on the removal of Pb^{2+} and Zn^{2+} ions was studied using an initial concentration of 10, 30, and 50 mg.L^{-1} for two metals and adjusting the pH of the solutions to 3.0, 4.0, and 5.0. These values were selected based on previous works

[24, 32]. This was made to determine whether there was a significant effect from concentration and pH, as well as from the interactions between these factors through analysis of variance (ANOVA) using Minitab 19.0 software [33].

Batch adsorption studies: heavy metal adsorption kinetics and isotherms were determined from batch experiments with constant stirring [34]. The adsorption rate of clay minerals gradually increases with increasing contact time then remains constant until equilibrium is attained. Most authors reported a time of 1-5 h for the adsorption process in the laboratory [35-38], although a few researchers [38] achieved complete uptake of the heavy metal species after 6 h contact time. Based on reports from the literature, the ideal temperature for adsorption of heavy metals is the room temperature, though slightly lower or higher temperatures ranging from 22 to 29 °C may still be ideal [38, 39]. The lead and zinc sources used in this work were lead nitrate [$Pb(NO_3)_2.6H_2O$] or zinc nitrate hexahydrate [$Zn(NO_3)_2.6H_2O$], both from Vetec Química. These reagents were dissolved in deionized water to prepare lead and zinc solutions with different initial concentrations (10, 30, and 50 mg.L^{-1}). These solutions (50 mL) were put in contact with 0.5 g of clay in Erlenmeyer flasks and pH of 3, 4, and 5. The contents were mixed on a shaking table (Braun Certomat MO, Biotech Int.) at 200 rpm (25 °C) for 5 h. The pH of the solutions was measured at the beginning and the end of each experiment and was adjusted when needed to avoid causing the chemical precipitation of metal species. After 5 h, the supernatants were sampled to determine the Zn(II) concentration and Pb(II) concentration using an atomic absorption spectrometer (AA Analyst 200, Perkin Elmer). The adsorption capacity of heavy metal at equilibrium (q_{eq}) was calculated by:

$$q_{eq} = \frac{V}{m} (C_0 - C_{eq}) \qquad\qquad (A)$$

where C_0 is the initial concentration (mg.L^{-1}), C_{eq} is the final concentration (mg.L^{-1}), q_{eq} is the removal capacity of the heavy metal at equilibrium (mg of metal/g of adsorbent), V is the solution volume (mL), and m is the adsorbent mass (g).

Equilibrium studies: adsorption isotherms: to obtain the equilibrium isotherms, 100 mL of solutions with different lead or zinc initial concentrations (50-160 mg.L^{-1}) were mixed with 1.0 g of clay under 200 rpm stirring rate for 5 h with pH maintained at 5.0 and temperature of 25 °C. *Kinetics studies*: the adsorption kinetics tests were carried using a finite bath system with a concentration of 50 mg.L^{-1} and a pH of 5.0. The tests consisted of three 2000 mL capacity beakers containing 1000 mL of solutions at a constant temperature of 25 °C under constant stirring, with a mixture at a ratio of 1/100 of clay mass/volume solution of lead nitrate or zinc nitrate. Aliquots from the solution were collected at different time intervals between 1 and 70 min, taking care that the withdrawn volume did not exceed 8% of the total volume.

RESULTS AND DISCUSSION

Clay properties: the X-ray diffraction (XRD) patterns

of the natural and thermally activated Chocolate B clay samples are presented in Fig. 1. The X-ray diffractogram of the natural Chocolate B clay (Fig. 1a) showed peaks characteristic of smectite clay (peak corresponding to an interplanar spacing, d_{001}, of 15.60 Å), the main clay minerals being smectite with the presence of some kaolinite and quartz [40, 41]. A low amount of kaolinite was detected at 4.57 Å. The diffractogram indicated a predominance of peaks for quartz as a clay impurity from 4.34 to 3.44 Å, confirming a substantial amount of silica in the clay [42]. The most common method to physically modify a ceramic material is through thermal treatment. The structure and composition of clay minerals can be modified by heating at high temperatures [43]. On heating, all clay minerals pass through a temperature range in which they are dehydrated to various degrees. In the upper region of this temperature range, dehydration and dehydroxylation may overlap. Dehydration causes changes that can be controlled and utilized [44]. As presented in Fig. 1b, the peak equivalent to the clay mineral smectite decreased in intensity after heating from 25 to 500 °C. The peak position of the smectite shifted to the right, and the d value decreased from 1.56

to 0.96 nm after thermal treatment. This result indicated a partial breakdown of the crystalline structure [45].

Table I presents the results from the X-ray fluorescence spectroscopy (XRF). The analysis seeks to identify the chemical constituents present in the sample in the form of oxides. It was clear that the Chocolate B clay was composed primarily of oxides of silicon, aluminum, and iron, from the presence of the clay minerals quartz, kaolinite, and smectite, respectively. The presence of a significant amount of Al_2O_3 in the sample (14.9%) was mostly Al that is combined in the structure with an exchangeable cation derived from the clay minerals in the samples [39]. The presence of Al and Si oxides as the principal components indicates that the material is aluminosilicate [46]. Fe_2O_3 was also found in significant amounts in Chocolate B clay, showing the clay was rich in iron. Oxides of calcium and magnesium were found in the clay at contents below 2%. Magnesium and calcium present in the sample are generally in the form of oxides as exchangeable cations [47, 48]. These chemical elements contribute to the high cation exchange capacity of the clay [46]. Comparing the composition of both samples, only slight differences were observed. Thus, the thermal treatment did not significantly alter the composition of the Chocolate B clay thermally activated at 500 °C.

Table II shows the results of surface area and volume of micropores and mesopores of the Chocolate B clay samples. Chocolate B clay had a specific surface area (S_{BET}) of 82 $m^2.g^{-1}$, a value typical of Brazilian smectite clays [49]. This value was similar to the value obtained for Brasgel clay, which was 73 $m^2.g^{-1}$ [50]. The surface area also affects the ion exchange capacity of the material, because the higher the specific surface area, the greater the number of sites on the surface of the material and, consequently, the higher its ion exchange capacity [51]. The thermal activation of Brasgel clay in a range of 100 to 500 °C was studied. Values of 73 $m^2.g^{-1}$ were found for raw Brasgel and 75 $m^2.g^{-1}$ for calcined Brasgel (300 °C) [41]. Thermally activated Chocolate B clay had an S_{BET} of 59 $m^2.g^{-1}$. Moreover, the specific surface area results revealed that there was a slight decrease from the natural clay to the thermally activated clay. The difference could be attributed to the loss of structural water.

Fig. 2 shows the N_2 adsorption isotherms of natural and thermally activated Chocolate B clays. They show the classic
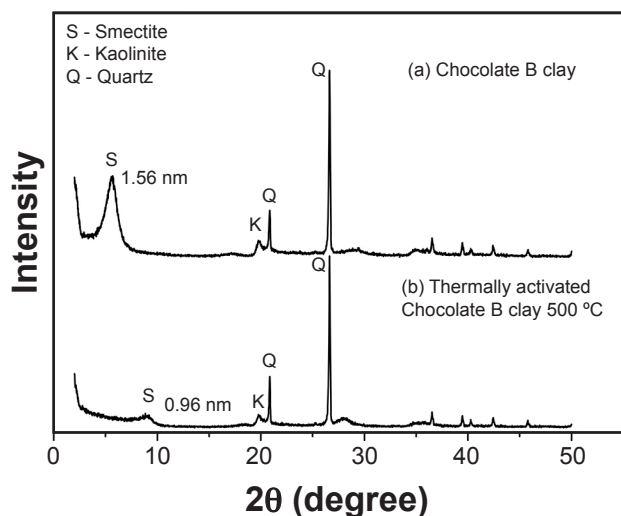

Figure 1: XRD patterns of natural (a) and thermally activated (500 °C) (b) Chocolate B clay samples.

Table I - Chemical composition (wt%) of the samples.

Chocolate B clay	SiO_2	Al_2O_3	Fe_2O_3	CaO	MgO	Impurities
Natural	69.4	14.9	9.1	2.0	1.7	2.9
Thermally activated	68.2	13.8	8.9	1.9	1.8	2.7

Table II - Textural analysis of the samples.

Chocolate B clay	S_{BET} ($m^2.g^{-1}$)	$V_{micropores}$ ($cm^3.g^{-1}$)	$V_{mesopores}$ ($cm^3.g^{-1}$)
Natural	82	0.0124	0.0559
Thermally activated 500 °C	59	0.0097	0.0387

shape of a type II adsorption isotherm, characteristic of the formation of multiple layers of adsorbed molecules on the solid surface. This type of sigmoid isotherm is often found for solid or non-porous materials where pores are larger than micropore size, which explains the low micropore volume values [52]. Under low pressure (P/P_0= 0 to 0.2), the adsorption occurs on the outer surface of the particles and surface micropores, if such pores (diameter 0-2 nm) exist. At higher relative pressure ($0.4<P/P_0<0.95$), the second and third adsorption layer is accompanied by condensation in mesopores (4-40 nm). Finally, at relative pressure >0.95, condensation in macropores (40 nm) occurs [53].
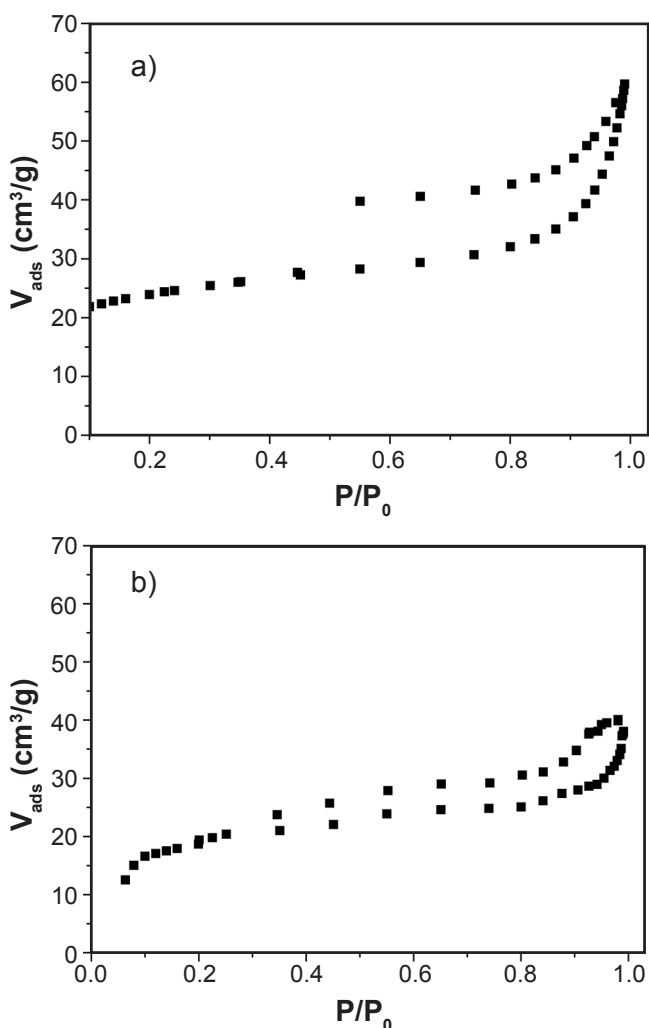

Figure 2: The adsorption and desorption isotherms of N_2 at liquid nitrogen of natural (a) and thermally activated (500 °C) (b) Chocolate B clay.

Determining the cation exchange capacity is useful for montmorillonites, vermiculite, and for other groups of clay minerals, alone or mixed with inert minerals, because it can uniquely identify the type of material present [40]. Cation exchange capacity (CEC) and specific surface area (SSA) are important properties of clay minerals that determine their adsorption capability. CEC is the total negative charges present in the clay which can attract and hold heavy metal cations [53]. The CEC for Chocolate B clay was 76 meq/100 g of clay, which is within the limits that pertain to the group of smectites, according to the literature [48, 54], and the CEC for thermally activated Chocolate B clay was 52 meq/100 g of clay.

Evaluation of the potential of Chocolate B clay for removing Pb^{2+} and Zn^{2+} using a batch system: the removal amount increased as the initial metal concentration was increased until the available adsorption sites became saturated [55]. The pH of the aqueous solution is considered an important variable that controls cationic adsorption onto the clay surface. This is due to the change in clay surface properties and the metal species with increased pH [56]. Table III lists results from the experimental design 2^2+3 center points for natural Chocolate B clay. The best adsorption capacity results were obtained in test 4 for the two metals studied, 3.36 and 3.72 mg.g^{-1} for lead and zinc, respectively. The best results for adsorption capacity (q_{eq}) were observed in the experiments with a pH of 5.0. In this pH range (3.0-5.0), the effect of precipitation of metals (Pb^{2+}, Zn^{2+}) in the form of hydroxides is reduced, and potential removal takes place by adsorption [57, 58]. The increased capacity for heavy metals when the pH increases may be attributed to the exchange adsorption of hydrolyzed species that compete for exchange sites with H$^+$ [59, 60].

Table III - Results from the experimental design 2^2+3 center points for natural and thermally activated Chocolate B clays (experimental conditions: initial concentration of 50 mg/L and pH 5.0).

Test	Variables		q_{eq} (mg/g) - natural		q_{eq} (mg/g) - thermally activated	
	C_i (mg/L)	pH	Pb^{2+}	Zn^{2+}	Pb^{2+}	Zn^{2+}
1	10	3	0.44	0.60	0.52	0.39
2	50	3	3.33	2.83	4.19	1.69
3	10	5	0.49	0.73	0.85	0.71
4	50	5	3.36	3.72	6.79	3.35
5	30	4	2.07	2.07	3.22	1.82
6	30	4	2.05	2.01	3.29	1.72
7	30	4	2.06	2.04	3.08	1.87

The main and interaction effects were evaluated considering a statistical significance at 95% confidence level [61]. The adsorption capacity models of lead and zinc and regression equations for natural clay are, respectively:

$$q_{eq,Pb} = -0.3650+0.07300Ci+0.02750pH-0.000250Ci*pH+0.15500PtCt \quad (B)$$

$$q_{eq,Zn} = 0.133+0.02725Ci-0.0300pH+0.009500Ci*pH+0.0700PtCt \quad (C)$$

Table IV - Results of analysis of variance (ANOVA) for the statistic model obtained for adsorption capacity onto natural and thermally activated Chocolate B clay.

Source	df	Natural Chocolate B clay						Thermally activated Chocolate B clay					
		q_{eq} - Pb^{2+} R^2=100.00%; R^2_{adj}=99.99%			q_{eq} - Zn^{2+} R^2=99.98%; R^2_{adj}=99.93%			q_{eq} - Pb^{2+} R^2=99.91%; R^2_{adj}=99.74%			q_{eq} - Zn^{2+} R^2=99.79%; R^2_{adj}=99.36%		
		Sum of squares	Mean square	p-value	Sum of squares	Mean square	p-value	Sum of squares	Mean square	p-value	Sum of squares	Mean square	p-value
Main effects	2	8.29	4.14	0.000	7.07	3.54	0.000	25.23	12.61	0.001	4.86	2.43	0.004
Interaction	1	0.00	0.00	0.000	0.14	0.14	0.006	1.29	1.29	0.009	0.45	0.45	0.013
Curvature	1	0.04	0.04	0.002	0.01	0.01	0.093	0.02	0.02	0.313	0.12	0.12	0.044
Pure error	2	0.00	0.00	-	0.002	0.002	-	0.02	0.01	-	0.01	0.01	-
Total	6	8.33	-	-	7.23	-	-	26.56	-	-	5.44	-	-

The models indicated that the system was strongly dependent on pH, contributing positively to the capacity of heavy metals. Table IV lists results of analysis of variance (ANOVA) for the statistic model obtained for adsorption capacity onto natural Chocolate B clay. The adjusted correlation coefficient was R^2=99.99% for Pb^{2+} and R^2=99.93% for Zn^{2+} indicating that model equations were satisfactory.

For modified clay, the best results were obtained in assays carried out under higher heavy metal concentrations, the best result being again that of test 4, with the removal of 6.79 mg of Pb^{2+}/g of clay and 3.35 mg of Zn^{2+}/g of clay. From these results, there was a greater affinity of modified Chocolate B clay with lead metal in relation to zinc metal (Table III). It can also be observed that experiments 1 and 2 showed the lowest removal potentials, due to the chosen pH (3), because, according to Inglezakis et al. [62], the more acidic the solution, the greater is the competition between the H^+ ions and the ions of the transition metals to be adsorbed, which makes their adsorption difficult. The main and interaction effects were evaluated considering a statistical significance at a 95% confidence level [61]. For the adsorption capacity, the initial concentration had a strong influence, with the best results occurring (q_{eq}) for the highest concentration level (C_0=50 mg.L^{-1}), with little influence from the pH. It appears that the statistical data, therefore, corroborated the results of the experimental design for the adsorption capacity of Pb^{2+} and Zn^{2+}. The adsorption capacity models of lead and zinc and regression equations for modified clay are, respectively:

$$q_{eq,Pb} = -0.041+0.0066C_0-0.1188pH+0.02838C_0pH+0.1092PtCt \qquad (D)$$

$$q_{eq,Zn} = 0.088-0.01775C_0-0.0075pH+0.01675C_0pH+0.2683PtCt \qquad (E)$$

The models indicated that the system was strongly dependent on pH, contributing positively to the capacity of heavy metal (Table IV lists ANOVA for the statistic model

obtained for adsorption capacity onto thermally activated Chocolate B clay). The adjusted correlation coefficients were R^2=99.74% for Pb^{2+} and R^2=99.36% for Zn^{2+} indicating that model equations were satisfactory. The chemical composition of Chocolate B clay was not modified by thermal activation, but the cation exchange capacity (CEC) and the specific surface area were reduced. Therefore, Chocolate B clay was selected for the equilibrium and the kinetic studies. Adsorption by various materials is often studied as a potential tool for the purification of water and industrial effluents. In general, works in this field report experimental results about the adsorption capacity of solutes at equilibrium, and about the kinetics of adsorption. The data are then described using various models or empirical formulas. Freundlich and Langmuir isotherms were selected because they are classic models in the literature.

Adsorption isotherms: the equilibrium isotherm represents the distribution of the adsorbed material between the adsorbed phase and the solution phase at equilibrium. The adsorption equilibrium isotherms are some of the most important data because they help clarify the mechanism of the adsorption process. The affinity between the amount of ions adsorbed on the clay and its equilibrium concentration in an aqueous solution was evaluated using the Langmuir model and Freundlich isotherms. The Langmuir model is suitable for characterizing the monolayer adsorption with the basic assumption that the adsorption occurs at specific sites and that the adsorbent is homogeneous [63]. The Freundlich isotherm, on the other hand, applies generally to non-specific adsorption systems with heterogeneous surfaces where multilayer adsorption can occur [64]. The mathematical expression representing the Langmuir isotherm is given by

$$q_{eq}= \frac{q_e.C_e}{K_L + C_e} \qquad (F)$$

where q_e is the maximum amount of adsorption with complete monolayer coverage on the adsorbent surface

(mg.g^{-1}), and K$_L$ is the Langmuir constant related to the energy of adsorption (L.mg^{-1}). Eq. G shows the Freundlich isotherm model:

$$q_{eq} = K_F.C_e^{1/n} \qquad (G)$$

where K$_F$ and n are the Freundlich adsorption-isotherm constants, indicating the extent of adsorption and the degree of nonlinearity between solution concentration and adsorption.

The non-linear models of Langmuir and Freundlich were fitted to the experimental equilibrium data, and the results are shown in Fig. 3. It can be seen that the equilibrium data for Chocolate B clay in the adsorption of metals Pb^{2+} and Zn^{2+} were adjusted for both Langmuir and Freundlich, which is consistent with the observation made by others [65]. The parameters obtained for the non-linear Langmuir-Freundlich equations are shown in Table V. Compared to some other adsorbents, such as Bofe clay with a q$_{max}$ of 4.39 mg.g^{-1} [66], and a lateritic clay with a q$_{max}$ of 5.60 mg.g^{-1} [67], both for heavy metals adsorption from aqueous solution, the values for maximum adsorption capacity for Zn^{2+} obtained in this study were superior. Table V shows the calculated values of the Langmuir and Freundlich model parameters. The Langmuir adsorption maxima q$_m$ were determined to be 19.85 and 12.64 mg/g for Pb^{2+} and Zn^{2+}, respectively. Mellah and Chegrouche [68] used natural bentonite for the elimination of Zn(II) from an aqueous solution.

The process was favored by high values of initial Zn(II) concentration and reduced particle size of clay adsorbent. It was also observed that process performance was strongly dependent on the agitation speed.

Kinetic studies: to determine the kinetics of the adsorption process, there are several models determining the adsorption kinetics. In this study, the data were adjusted to the pseudo-second-order [69, 70]. From the results, it was found that the Pb^{2+} and Zn^{2+} sorption rates were relatively fast for the first 10 min. Following this stage, a slow adsorption process took place and the equilibrium was then attained at approximately 30 min. Diffusional restrictions are very important in these processes. One or more mechanistic steps may be involved: 1) external mass transport, 2) diffusional mass transfer within the internal structure of the adsorbent particle, and 3) adsorption at sites located at the surface. The first step is not rate-limiting since the effect of transport in the solution can be eliminated by efficient mixing. The second step must be reduced in clay minerals, because these materials expand in the presence of large amounts of water, promoting complete separation of the unit layers. Adsorption rate prediction provides information for selecting optimal operating conditions in large-scale batch processes. To investigate the mechanism of adsorption kinetics, we used the pseudo-first-order and pseudo-second-order models developed by Ho and McKay [71, 72]. The pseudo-first-order model is represented by the equation rearranged to
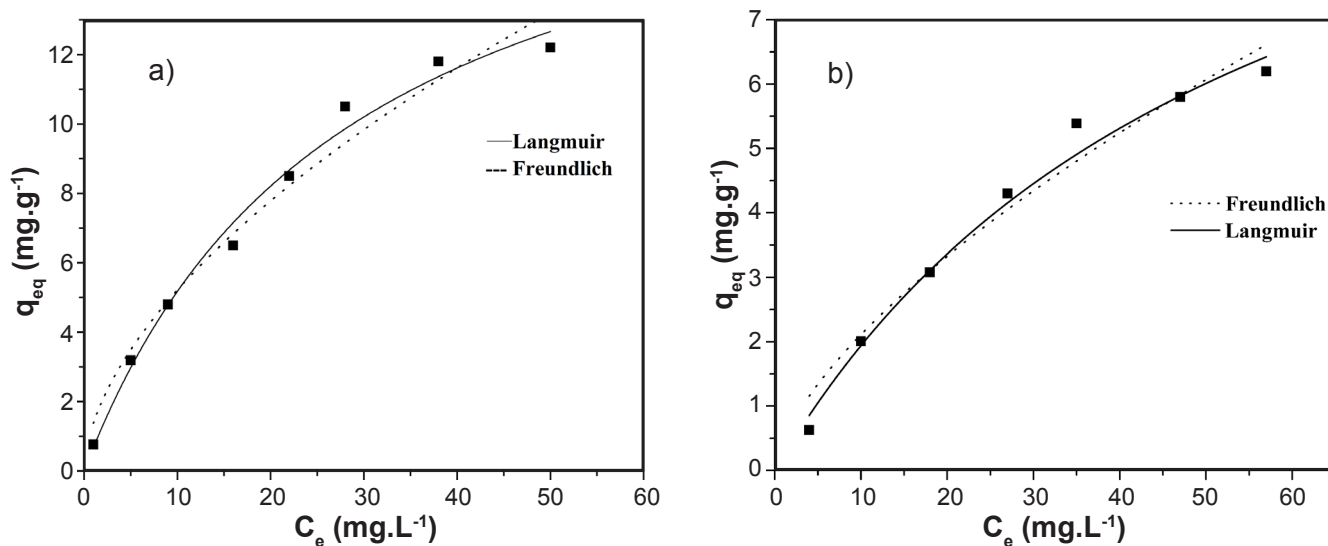

Figure 3: Adsorption isotherms of Pb^{2+} (a) and Zn^{2+} (b) using Chocolate B clay and non-linear adjustments: Langmuir and Freundlich.

Table V - Isothermal parameters of non-linear adjustments of Langmuir and Freundlich.

Metal	Langmuir parameters			Freundlich parameters		
	q$_m$ (mg.g^{-1})	K$_L$ (L.mg^{-1})	R^2	K$_F$ (g.L^{-1})	n	R^2
Pb^{2+}	19.85	0.0352	0.989	1.376	1.729	0.975
Zn^{2+}	12.64	0.0181	0.994	0.466	1.524	0.967

the linear form:

$$q_t = q_{eq}[1-\exp(k_1.t)] \qquad (H)$$

The model of the pseudo-second-order according to Ho and McKay [73] is given by:

$$\frac{t}{q_t} = \frac{1}{k_2 q_{eq}^2} + \frac{1}{q_{eq}} t \qquad (K)$$

where q_{eq} is the amount of heavy metal adsorbed at equilibrium (mg.g^{-1}), q_t is the amount of heavy metal adsorbed at any given time (mg.g^{-1}), k_1 and k_2, respectively, are the equilibrium rate constants of pseudo-first-order adsorption (min^{-1}) and pseudo-second-order adsorption (g.mg^{-1}.min^{-1}), t is the time (min), and $k^2 q_{eq}^2$ is the initial adsorption rate when $t \to 0$.

The experimental data adjusted to the first- and second-order models are presented in Fig. 4. The adsorption speed was seen to be high at the beginning of the process for the two metals, reaching equilibrium in approximately 10 min for the two systems. This rapid adsorption is probably due to a large number of adsorption sites available on the
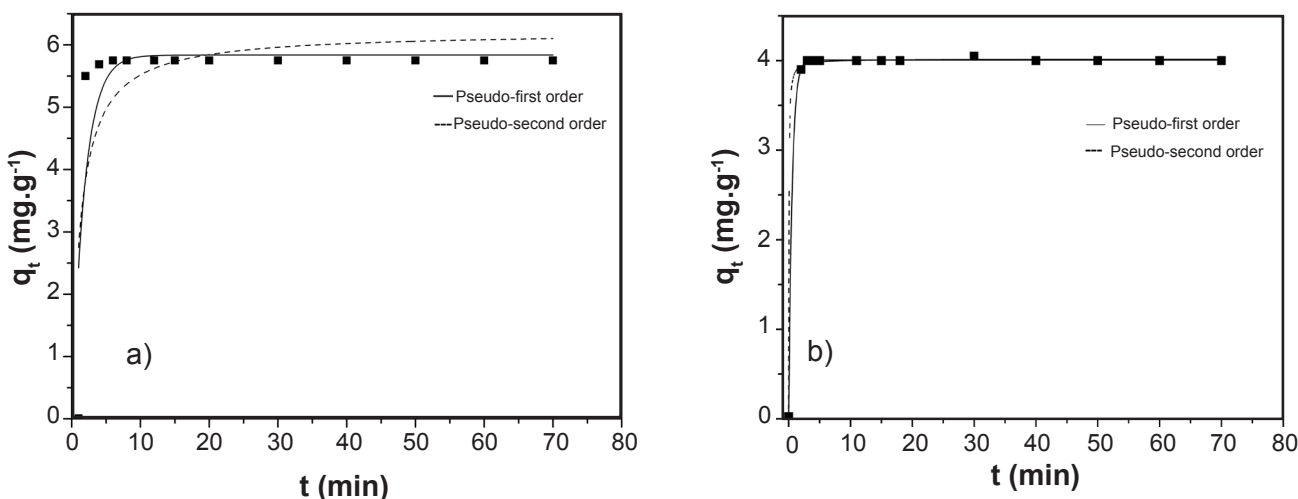

Figure 4: Adsorption kinetics of Pb^{2+} (a) and Zn^{2+} (b) onto Chocolate B clay and non-linear fits: pseudo-first-order and pseudo-second-order.

Table VI - Kinetic parameters of pseudo-first-order and pseudo-second-order models.

Metal	Pseudo-first order			Pseudo-second order		
	q_{eq} (mg.g^{-1})	K_1 (min^{-1})	R^2	q_{eq} (mg.g^{-1})	K_2 (g.mg^{-1}.min^{-1})	R^2
Pb^{2+}	5.83	0.537	0.704	6.21	0.128	0.593
Zn^{2+}	4.00	1.826	0.999	4.02	6.348	0.999

Table VII - Heavy metal removal data by sorption using different adsorbents.

Sorbent	Heavy metal	Parameters	q_{eq} (mg/g)	Ref.
Chocolate B clay	Pb^{2+}	C_0 (10, 30, 50 mg.L^{-1}), pH (3.0, 4.0, 5.0)	3.36	This work
	Zn^{2+}		3.72	
Gray clay	Zn^{2+}	Mechanical agitation (100 to 200 rpm), pH (6.0 to 8.0), C_0 (10 to 50 mg.L^{-1})	4.37	[35]
Chocobofe clay	Pb^{2+}	C_0 (10, 30, 50 mg.L^{-1}), pH (3.0, 4.0, 5.0)	3.36	[50]
Natural zeolite	Pb^{2+}		7.80	
	Ni^{2+}	C_0=20 mg.L^{-1}, pH=7.5	5.40	[75]
	Cu^{2+}		1.40	
Brasgel clay	Cd^{2+}	C_0 (10, 30, 50 mg.L^{-1}), pH (3.0, 4.0, 5.0)	2.63	[76]
Activated carbon	Cu^{2+}	C_0=100 to 500 mg.L^{-1}, pH=5.0, T=30 °C	4.00	[77]

clay surface. The kinetic experiment clearly indicated that adsorption of heavy metals (Pb^{2+} and Zn^{2+}) by Chocolate B clay was a process that happened in two steps: very rapid adsorption of heavy metal ions on the external surface was followed by a slower intraparticle diffusion into the interior of the adsorbent. This two-stage metal ion uptake can also be explained as adsorption occurring on two different types of binding sites on the adsorbent particles. Rapid kinetics has significant practical implications, as it facilitates the use of smaller reactor volumes, ensuring high efficiency and economy [24, 74]. As shown in Fig. 4a, the pseudo-first-order model fitted the experimental data better than the pseudo-second-order kinetic model for the Chocolate B clay (Pb^{2+}). The correlation coefficient R^2 value for the pseudo-second-order model (0.704) was greater than that of the pseudo-first-order model. Fig. 4b shows the good fit of the models proposed by Sprynskyy et al. [75], with R^2 values of 0.999 and 0.999 for Chocolate B clay (Zn^{2+}). The calculated kinetic parameters for the pseudo-first-order and pseudo-second-order models of Pb^{2+} and Zn^{2+} on Chocolate B clay, with an initial concentration of 50 mg.g^{-1}, are listed in Table VI. The second-order behavior indicated that the process was essentially controlled by the diffusion of zinc species into pores, which exemplifies that second-order kinetic models can be successfully used in order to describe interactions that take place during metal adsorption into the clay pores [35].

Adsorption capacities of Zn^{2+} and Pb^{2+} for the adsorbent used in the present work were compared with those of other adsorbents reported in the literature (Table VII). Based on the removal of heavy metals, the Chocolate B clay was efficient, with values of q_{eq} of 3.36 mg.g^{-1} for Pb^{2+} and 3.72 mg.g^{-1} for Zn^{2+}. Similar results were found elsewhere [35, 50, 75-77]. Although traditional adsorbents such as zeolites and activated carbon present higher q_{eq} values, we can affirm that Chocolate B clay has a reasonable adsorption capacity. The use of clays as adsorbents has advantages over many other commercially available adsorbents (in this case, zeolite and activated carbon) in terms of low cost, abundant availability, high specific surface area, excellent adsorption properties, non-toxic nature, and large potential for ion exchange.

CONCLUSIONS

The chemical composition of Chocolate B clay was not modified by thermal activation, but the cation exchange capacity (CEC) was reduced. The N_2 physisorption isotherms obtained can be classified as type II or BET, characteristic of multilayered formation composed of adsorbed molecules on the solid surface, typical of non-porous solids or pores greater than the micropores. Thermal activation caused the reduction of the surface area. Both natural and thermally activated Chocolate B clays possessed a high affinity for the two heavy metals (Pb^{2+} and Zn^{2+}). The effects of process parameters such as pH and initial concentration were studied. The most significant effect was found to be pH. This work presented an equilibrium study of the adsorption of

Pb^{2+} and Zn^{2+} in the Chocolate B clay, which is important to comprehend and analyze the entire process. The Langmuir isotherm model provided the best fit for the experimental adsorption data for Pb^{2+} and Zn^{2+} ions. Kinetic models of pseudo-first-order and pseudo-second-order were fitted to experimental data. For the Chocolate B clay system with Zn^{2+}, the two models fitted well, but for the Chocolate B clay system with Pb^{2+}, the pseudo-first-order model fitted better.

REFERENCES

[1] K.H. Vardhan, P.S. Kumar, R.C. Panda, J. Mol. Liq. **290** (2019) 111197.
[2] S.H. Awa, T. Hadibarata, Water Air Soil Pollut. **231** (2020) 47.
[3] S. Babel, E.M. Opiso, Int. J. Environ. Sci. Technol. **4** (2007) 99.
[4] C.O. Nwuche, E.O. Int. J. Environ. Sci. Technol. **3** (2008) 409.
[5] T. Hongo, S. Yoshino, A. Yamazaki, A. Yamasaki, S. Satokawa, Appl. Clay Sci. **70** (2012) 74.
[6] M.M. Barbooti, J. Environ. Prot. **6** (2015) 237.
[7] D.M. Ruthven, *Principals of adsorption and adsorption processes*, John Wiley Sons, New York (1984).
[8] G.Z. Kyzas, G. Bomis, R.I. Kosheleva, E.K. Efthimiadou, E.P. Favvas, M. Kostoglou, A.C. Mitropoulos, Chem. Eng. J. **356** (2019) 91.
[9] A. Maleki, B. Hayati, F. Najafi, F. Gharibi, W.J. Sang, J. Mol. Liq. **224** (2016) 95.
[10] B. Hayati, A. Maleki, F. Najafi, H. Daraei, F. Gharibi, G. McKay, J. Mol. Liq. **237** (2017) 428.
[11] R. Ebrahimi, B. Hayati, B. Shahmoradi, R. Rezaee, M. Safari, A. Maleki, K. Yetilmezsoy, Environ. Technol. Innov. **12** (2018) 261.
[12] L. Giraldo, A. Erto, J.C. Moreno-Piraján, Adsorption **19** (2013) 465.
[13] K. Simeonidis, C. Martinez-Boubeta, P. Zamora-Perez, P. Rivera-Gil, E. Kaprara, E. Kokkinos, M. Mitrakas, in "Environmental nanotechnology", N. Dasgupta, S. Ranjan, E. Lichtfouse (Eds.), Springer (2018) 75.
[14] K. Li, N. Miwornunyuie, L. Chen, H. Jingyu, P.S. Amaniampong, D.A. Koomson, D. Ewusi-Mensah, W. Xue, G. Li, H. Lu, Sustainability **13** (2021) 984.
[15] S. Mnasri-Ghnimi, N. Frini-Srasra, Appl. Clay Sci. **179** (2019) 105151.
[16] D. Ozdes, C. Duran, H.B. Senturk, J. Environ. Manage. **92** (2011) 3082.
[17] T. Zhang, W. Wang, Y. Zhao, H. Bai, T. Wen, S. Kang, G. Song, S. Song, S. Komarneni, Chem. Eng. J. **420** (2020) 127574.

[18] V.B. Yadav, R. Gadi, S. Kalra, J. Environ. Manage. **232** (2019) 803.

[19] S. Gu, X. Kang, L. Wang, E. Lichtfouse, C. Wang, Environ. Chem. Lett. **17** (2019) 629.

[20] M.K. Uddin, Chem. Eng. J. **308** (2017) 438.

[21] B.O. Otunola, O.O. Ololade. Environ. Technol. Innov. **18** (2020) 100692.

[22] R.Y. Stefanova, J. Environ. Sci. Health B **3** (2001) 293.

[23] S.T. Akar, Y. Yetimoglu, T. Gedikbey, Desalination **244** (2009) 97.

[24] M.L.P. Silva, M.G.F. Rodrigues, M.G.C. Silva, Cerâmica **55**, 333 (2009) 11.

[25] J.D. Mota, "Modificação e caracterização de argila esmectita Chocolate B visando seu uso no processo de tratamento de águas contaminadas por metais pesados", M.Sc. Diss., UFCG, Campina Grande (2013).

[26] H.D. Chapman, in "Methods of soil analysis part 2: chemical and microbiological properties", A.G. Norman (Ed.), Am. Soc. Agron., Madison (1965) 891.

[27] G.J. Churchman, W.P. Gates, B.K.G. Theng, G. Yuan, Dev. Clay Sci. **1** (2006) 625.

[28] C. Chen, H. Liu, T. Chen, D. Chen, R.L. Frost, Appl. Clay Sci. **118** (2015) 239.

[29] Es-Shahbany, M. Berradi, M. Belfakir, M.S. El Youbi, Mor. J. Chem. **4** (2016) 352.

[30] D. Mohapatra, D. Mishra, G.R. Chaudhury, R.P. Das, Korean J. Chem. Eng. **24**, 3 (2007) 426.

[31] J.H. Potgieter, S.S. Potgieter-Vermaak, P.D. Kalibantonga, Miner. Eng. **19**, 5 (2006) 463.

[32] J.V.N. Silva, "Remoção de metais pesados (Cd, Pb, Zn) utilizando como adsorventes argilas nacionais: Chocobofe e Chocolate B", Doct. Thesis, UFCG, Campina Grande (2015).

[33] Minitab Statistical Software, Data Analysis Software, v.19 (2019).

[34] C. Tien, *Adsorption calculation and modeling*, Butteworth-Heinemann, Boston (1994).

[35] P.N.M. Vasconcelos, W.S. Lima, M.L.P. Silva, A.L.F. Brito, H.M. Laborde, M.G.F. Rodrigues, Am. J. Anal. Chem. **4** (2012) 510.

[36] C. Green-Ruiz, Environ. Technol. **30**, 1 (2009) 63.

[37] W.M. Gitari, Toxicol. Environ. Chem. **96**, 2 (2014) 201.

[38] H. Es-Sahbany, M. Berradi, S. Nkhili, R. Hsissou, M. Allaoui, M. Loutfi, M.S. El Youbi, Mater. Today Proc. **13** (2019) 866.

[39] F. Moyo, R. Tandlich, B. Wilhelmi, S. Balaz, Int. J. Environ. Res. Public Health **11**, 5 (2014) 5020.

[40] P. Souza Santos, *Ciência e tecnologia de argilas*, 2nd ed., Edgard Blücher, São Paulo (1992).

[41] C.F. Gomes, *Argilas: o que são e para que servem*, Fund. Calouste Gulbenkian, Lisboa (1988).

[42] S. Wang, E. Ariyanto, J. Coll. Interface Sci. **314** (2007) 25.

[43] F. Hussin, M.K. Aroua, W.M.A.W. Daud, Chem. Eng. J. **170** (2011) 90.

[44] L. Heller-Kallai, in "Handbook of clay science", F. Bergaya, B.K.G. Theng, G. Lagaly (Eds.), Elsevier (2006) 289.

[45] M.J. Rezende, A.C. Pinto, Renew. Energy **92** (2016) 171.

[46] M. Vhahangwele, G.W. Mugera, J. Environ. Chem. Eng. **3** (2015) 2425.

[47] M.F.G. Rodrigues, Cerâmica **49**, 311 (2003) 146.

[48] R.E. Grim, *Clay mineralogy*, McGraw-Hill, New York (1968).

[49] G.C. Oliveira, M.F. Mota, M.M. Silva, M.G.F. Rodrigues, H.M. Laborde, Braz. J. Pet. Gas **6** (2012) 171.

[50] W.S. Lima, A.L.F. De Brito, M.G.F. Rodrigues, M.F. Mota, M.M. Silva, Mater. Sci. Forum **805** (2015) 662.

[51] L. Michot, F. Villieras, in "Handbook of clay science", F. Bergaya, B.K.G. Theng, G. Lagaly (Eds.), Elsevier (2006) 965.

[52] D.M. Ruthven, *Principals of adsorption and adsorption processes*, John Wiley Sons, New York (1984).

[53] T. Al-Ani, O. Sarapää, "Clay and clay mineralogy: physical-chemical properties and industrial uses", Geological Survey of Finland (2008).

[54] V.A. Weiss, Chemie **297** (1958) 257.

[55] A. Sdiri, T. Higashi, T. Hatta, F. Jamoussi, N. Tase, Chem. Eng. J. **172**, 1 (2011) 46.

[56] S. Mnasri-Ghnimi, N. Frini-Srasra, Appl. Clay Sci. **179** (2019) 105151.

[57] J.V.N. Silva, J.R. Scheibler, M.G.F. Rodrigues, Mater. Sci. Forum **820** (2015) 539.

[58] A. Kaya, A.H. Oren, J. Hazard. Mater. **125** (2005) 183.

[59] I. Ghorbel-Abid, M. Trabelsi-Ayadi, Arab. J. Chem. **8** (2011) 31.

[60] K.G. Tiller, in "Contaminants and the soil environment in the Australasia-Pacific Region", R. Naidu, R.S. Kookana, D.P. Oliver, S. Rogers, M.J. Mclaughlin (Eds.), Kluwer, Dordrecht (1996) 1.

[61] D.C. Montgomery, G.C. Runger, *Applied statistics and probability for engineers*, 3rd ed., John Wiley Sons, New York (2003).

[62] V.J. Inglezakis, M.A. Stylianou, D. Gkantzou, M.D. Loizidou, Desalination **210** (2007) 248.

[63] S. Arfaoui, N. Frini-Srasra, E. Srasra, Desalination **222** (2008) 474.

[64] H. Chen, A.Q. Wang, J. Coll. Interface Sci. **307** (2007) 309.

[65] R. Huang, B. Wang, B. Yang, D. Zheng, Z. Zhang, Desalination **280** (2011) 297.

[66] A.L.P. Araujo, M.L. Gimenes, M.A.S.D. Barros, M.G.C. Silva, Mater. Res. **16** (2013) 128.

[67] M. Sarkar, A.R. Sarkar, J.L. Goswami, J. Hazard. Mater. **149** (2007) 666.

[68] A. Mellah, S. Chegrouche, Water Res. **31** (1997) 621.

[69] D. Kumar, J.P. Gaur, Bioresour. Technol. **102** (2011) 633.

[70] L. Khezami, R. Capart, J. Hazard. Mater. **123** (2005) 223.

[71] Y.S. Ho, G. McKay, Trans. IchemE **76** (1998) 183.

[72] Y.S. Ho, G. McKay, Process Saf. Environ. Prot. **77** (1999) 165.

[73] Y.S. Ho, G. McKay, Process Biochem. **34** (1999) 451.

[74] M.X. Loukidou, A.I. Zouboulis, T.D. Karapantsios, K.A. Matis, Colloids Surf. A **242**, 1 (2004) 93.

[75] M. Sprynskyy, B. Buszewski, A.P. Terzyk, J. Namieśnik, J. Colloid Interface Sci. **304** (2006) 21.

[76] J.D. Mota, R.S.S. Cunha, P.N.M. Vasconcelos, M.G.F. Rodrigues, Mater. Sci. Forum **912** (2018) 202.

[77] P.S. Kumar, V. SathyaSelvaBala, K. Ramakrishnan, P. Vijayalakshmi, S. Sivanesan, Russ. Chem. Bull. **59** (2010) 185.